Effect of the Origin of ZnO Nanoparticles Dispersed in Polyimide Films on Their Photoluminescence and Thermal Stability

Anongnat Somwangthanaroj,[1] Chuthatai Phanthawonge,[1] Shinji Ando,[2] Wiwut Tanthapanichakoon[3]

[1]*Department of Chemical Engineering, Faculty of Engineering, Chulalongkorn University, Bangkok 10330, Thailand*
[2]*Department of Chemistry and Materials Science, Tokyo Institute of Technology, Tokyo 152-8552, Japan*
[3]*National Nanotechnology Center, National Science and Technology and Development Agency, Pathumtani 12120, Thailand*

Received 13 November 2007; accepted 26 February 2008
DOI 10.1002/app.28299
Published online 5 August 2008 in Wiley InterScience (www.interscience.wiley.com).

ABSTRACT: Polyimide (PI) films containing dispersed ZnO nanoparticles were prepared from both zinc nitrate hexahydrate (designated as $Zn(NO_3)_2$/PI) and ZnO nanoparticles, 2-nm average primary size (ZnO/PI). This work shows how the origin of ZnO affects both the photoluminescence and thermal decomposition of the film. The presence of ZnO derived from $Zn(NO_3)_2{\cdot}6H_2O$ was confirmed by X-ray diffraction technique. The fluorescent intensities from $Zn(NO_3)_2$/PI and ZnO/PI were much higher than that from pure PI films. When the ZnO concentration exceeded a certain saturation level, the emission intensity decreased due to the undesirable aggregation of ZnO. At the same concentration, ZnO/PI exhibited higher emission intensity than $Zn(NO_3)_2$/PI. All samples prepared under nitrogen emitted higher intensity than their counterparts prepared under argon. The ZnO/PI film was thermally more stable than the $Zn(NO_3)_2$/PI one. From TEM images of 117.6 mol% ZnO/PI films, the ZnO aggregates, whose average size was 17–90 nm, were well distributed throughout the film but poorly dispersed in nanometer range. J Appl Polym Sci 110: 1921–1928, 2008

Key words: fluorescence; polyimide; thermal properties; ZnO; nanoparticle

INTRODUCTION

Polyimide (PI) was firstly reported by DuPont Co in 1960s and has been widely-known with its trade name of Kapton.[1] It shows a variety of superior properties such as thermoxidative stability, high modulus, excellent electrical properties, and chemical resistance but also showed insufficient properties important for optoelectronics and display technology such as poor radiation durability against UV light, transparency, chemical, and thermal stability properties.[1] Introduction of fluorine atoms to PI improves several properties such as lower dielectric constants, higher thermal, and chemical stability, radiation durability against UV light, good transparency in the visible light and NIR regions, lower refractive indices, and lower glass transition temperature of polyimides.[1] As reported by numerous researches, fluorinated PIs have been typically prepared from 4,4′-(hexafluoroisopropyllidene) diphthalic anhydride (6FDA).[2–4] These 6FDA PIs show good transparency and lower dielectric constants than those prepared from other nonfluorinated dianhydrides.[1] The fluorinated PIs, which are suitable for optical light-emitting applications, exhibit high radiation durability in the UV (λ = 200–380 nm) region, high transparency in the visible (λ = 380–740 nm) and near infrared (NIR) regions (λ = 740–2500 nm).

Nanocrystals of semiconducting materials have been extensively studied in the past decade for use in light emitting diodes[5] and photovoltaic solar cells.[6] An *n*-type semiconductor with a band gap of 3.4 eV and an exciton binding energy of 60 meV, zinc oxide (ZnO) is a versatile material with many applications including antireflection coating, transparent electrodes in solar cells, gas sensors, varistors, light emitting diodes, and surface acoustic wave devices. At room temperature, ZnO emits ultraviolet (UV) luminescence,[7] and violet electroluminescence and blue light-emitting LED were successfully produced.[8] Therefore, much attention is now focused on the light emission properties of ZnO.

Combining ZnO nanoparticles with a polymer should enhance its optical properties such as fluorescence and radiation durability. ZnO/polymer

Correspondence to: A. Somwangthanaroj (anongnat.s@chula.ac.th).

Contract grant sponsors: Thailand Research Fund (TRF), Thailand-Japan Technology Transfer Project (TJTTP).

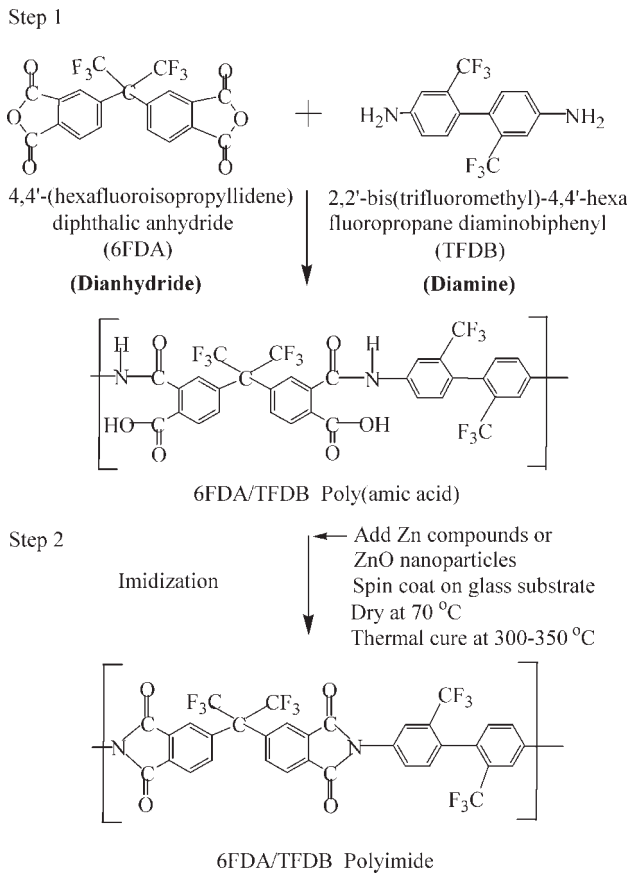

Figure 1 Chemical structures of monomers and preparation process of poly(amic acid) and polyimide.

composites have been produced with different polymer matrices, such as poly(vinyl pyrrolidone)[9] and poly (hydroxyethyl methacrylate).[10] Therefore we are interested in the uniform dispersion of ZnO in PI films because of the expected superior optical characteristics such as high fluorescence, high transparency, and high radiation durability, which are suitable for applications in optoelectronics, light emitting diodes, photonics and flat-panel display industries. This work shows how the origin of ZnO affects both the photoluminescence and thermal decomposition of the film.

EXPERIMENTAL

Materials

As shown in Figure 1, a fluorinated polyimide, 6FDA/TFDB, which exhibits good optical properties and high transparency, was synthesized from 4,4′-(hexafluoroisopropyllidene) diphthalic anhydride (6FDA) and 2,2′-bis(trifluoromethyl)-4,4′-hexafluoropropane diaminobiphenyl (TFDB). Monomers were purified by sublimation process before use. In this process, the dianhydride and diamine reacted in a dipolar aprotic solvent *N,N*-dimethylacetamide (DMAc) obtained from Aldrich Chemical. Zinc nitrate hexahydrate ($Zn(NO_3)_2{\cdot}6H_2O$) (99.9% purity) was also obtained from Aldrich Chemical. Zinc oxide nanoparticles with average primary diameters of about 2 nm were obtained from Meliorum Technologies, USA, and used as received.

Preparation of poly(amic acid) solution

As shown in Figure 1, 6 FDA/TFDB-PI was prepared by the reaction between 6FDA and TFDB, which have six fluorine atoms in both monomers. More specifically, 6FDA was completely dissolved in *N,N*-dimethylacetamide (DMAc) solvent to give a clear, colorless solution. Then an equimolar amount of TFDB was slowly added to the solution with stirring to obtain a 15 wt % poly(amic acid) (PAA) solution. The solution was gently stirred at room temperature for 24 h. Poly(amic acid), which contains carboxamide and carboxyl group was obtained from the reaction between dianhydride from 6FDA with diamine from TFDB as shown in Figure 1.

Preparation of the ZnO/PI films

Either $Zn(NO_3)_2{\cdot}6H_2O$ or ZnO nanopowder with an average primary diameter of about 2 nm was added into the above PAA solution at the desired molar concentration of ZnO. All the synthesizing and mixing procedures were performed in argon atmosphere. Then the PAA solution was spin coated onto a glass substrate at 1000–1500 rpm for 15 s to give a thin film. The film was dried at 70°C for 1 h in either nitrogen or argon atmosphere and thermally imidized at curing temperature in the range of 300–350°C for 1 h in either nitrogenor argon atmosphere, and then cooled down to room temperature. Note that there were two ways of preparing PI films embedded with ZnO nanoparticles. First, ZnO nanoparticles were added directly to the PAA solution. Then the PAA was imidized, and the resulting nanocomposite film was designated as ZnO/PI. In the second method $Zn(NO_3)_2{\cdot}6H_2O$ was added to the PAA solution and subsequently converted to ZnO at elevated temperatures with thermal imidization of PAA. The resulting nanocomposite film was designated as $Zn(NO_3)_2$/PI. Note that the concentration of ZnO in PI films was expressed as a percentage by mole of the ZnO comparing to the repeating unit of PI.

Measurements

The luminescent property of the films was characterized by a Luminescence Spectrometer (Perkin–Elmer LS 50) at room temperature using a xenon lamp as the light source. The wavelengths for excitation were

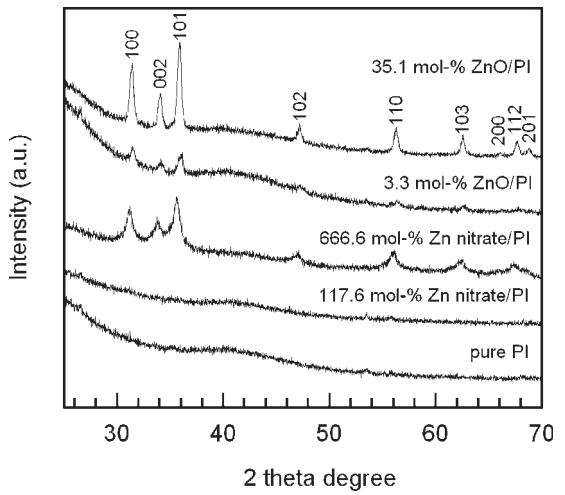

Figure 2 XRD patterns of pure PI, PI with ZnO nanoparticles from thermal decomposition of $Zn(NO_3)_2$ hexahydrate and ZnO nanoparticles directly added into PI.

in the range of 250–450 nm, and the fluorescent emission was detected in the range of 350–600 nm. The optical absorption property was characterized by a spectrophotometer (Hewlett–Packard 8452A diode array) at room temperature. The wide-angle X-ray diffraction measurements (XRD) were carried out at ambient temperature using a Siemens D500 diffractometer with Cu$K\alpha$ radiation and Ni filter in the 2θ range of 20°–70° with a resolution of 0.02° min^{-1}. The glass transition temperature was examined using a differential scanning calorimeter (DSC, diamond DSC Perkin-Elmer) between 50 and 460°C at a heating rate of 20°C min^{-1} under nitrogen atmosphere. Thermogravimetric analysis (TGA, TA Instruments SDT Q-600) was used to determine the degradation temperature at heating rate 20°C min^{-1} from 35 to 1000°C under nitrogen atmosphere. The transmission electron microscopy (TEM) image was taken with an electron microscope (JEOL, JEM-2100). The PI films were embedded in epoxy resin and sectioned into a thickness of 20 nm with an ultra microtome (ultrotome V).

RESULTS AND DISCUSSION

The XRD patterns of the PI films containing ZnO nanoparticles are shown in Figure 2. The characteristic XRD peaks, which correspond to the diffraction patterns of ZnO, indicated that ZnO crystallites are presented in the film.[11] The XRD pattern of 35.1 mol % ZnO/PI agrees well with the wurtzite ZnO hexagonal phase which is consistent with the standard values for bulk ZnO. In addition, the positions of the first three XRD peaks of both 3.3 mol % ZnO/PI and 666.6 mol % $Zn(NO_3)_2$/PI are clearly observed, thereby confirming the existence of the wurtzite ZnO hexagonal phase.

Though the 35.1 mol % ZnO/PI showed the distinct peaks indicating the presence of ZnO crystal in PI films, the XRD peaks of 3.3 mol % ZnO/PI showed smaller and broader peaks because of its lower concentration. Interestingly, the 35.1 mol % ZnO/PI film exhibited sharper peaks than the 666.6 mol % $Zn(NO_3)_2$/PI film. This could be attributed to an imperfect crystal structure and smaller crystallite sizes of ZnO in the film. Average size of ZnO nanoparticles (D) can be estimated using the Scherrer's formula as

$$D = \frac{0.9\lambda}{\beta\cos\theta} \quad (1)$$

where λ is the wavelength of the X-ray (1.5418°A), β is the line width at half height of the maximum peak and θ is Bragg angle of the diffraction peaks. The estimated D values are 13.5 and 5 nm for the 35.1 mol % ZnO/PI and the 666.6 mol % $Zn(NO_3)_2$/PI, respectively.

Though the 666.6 mol % $Zn(NO_3)_2$/PI film showed broad peaks with low intensity, it was confirmed that $Zn(NO_3)_2$ dissolved in PAA solution was successfully converted to ZnO nanoparticles by thermal decomposition. However, the 117.6 mol % $Zn(NO_3)_2$/PI film did not show any XRD peaks, which may be due to the small crystallite size, imperfect crystal structure and too little amount of ZnO below the detection limit of the diffractometer. This result is consistent with those of Sawada and Ando's[12] and Chiang and Whang's[13].

Figure 3 shows the DSC thermograph and the estimated glass transition temperatures (T_g) for the pure PI and ZnO/PI. The T_g of 0.6 and 3.3 mol % ZnO/PI films remained essentially the same as that of pure

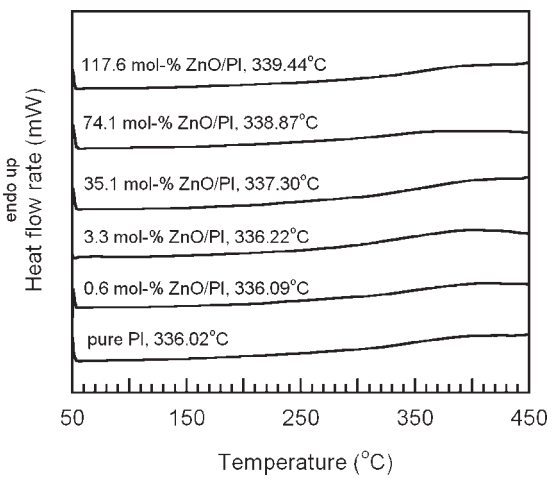

Figure 3 DSC heating thermograms of PI containing directly added ZnO nanoparticles.

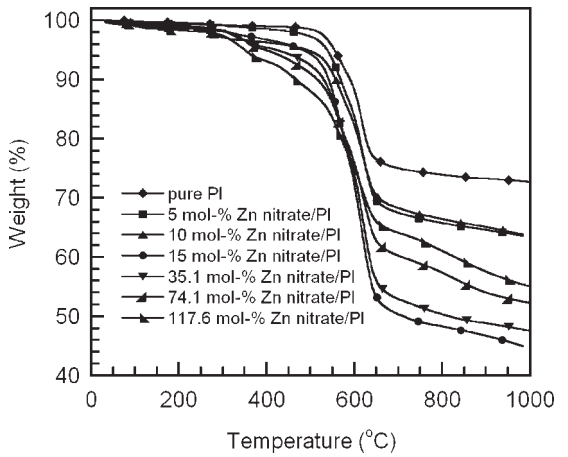

Figure 4 Thermogravimetric profiles of PI containing ZnO nanoparticles from thermal decomposition of $Zn(NO_3)_2$ hexahydrate.

PI, which was 336°C, whereas the T_g of 35.1, 74.1, and 117.6 mol % ZnO/PI slightly increased to 337.3, 338.9, and 339.4°C, respectively. This result is consistent with Hsu et al.'s [10] and Chae and Kim's[14]. Adding a solid filler into a polymer would reduce the mobility of the polymer chains, thereby resulting in an incremental increase in the T_g value.[15] There are two major causes to the reduction in the mobility of polymer chains in composites i.e., tethering and chain confinement.[14,15] The chain tethering is caused by the attractive forces between the filler surfaces and polymer chains. On the other hand, the chain confinement occurs when the mobility of polymer chains is significantly obstructed by the fillers. The T_g values of 35.1 mol % and higher concentration ZnO/PI slightly increased because of the chain confinement because there was little attractive force between the surface of ZnO and polymer chains.[14] By the way, T_g was not observed in the DSC thermographs of Zn nitrate/PI (data not shown). It could be ascribed to the formation of ZnO[12,13] during the combined decomposition and imidization of $Zn(NO_3)_2$/PI films. The brittleness of the film may be due to the chain scission caused by generated nitric acid or ions. In addition, the formation of ZnO may affect the mobility of polymer chain, which is reflected to the obscured glass transition in $Zn(NO_3)_2$/PI film.

The presence of ZnO nanoparticles in PI films also affected their degradation temperature (T_d), which is defined as the temperature of the samples at 5 wt % loss. It was found that the T_d of $Zn(NO_3)_2$/PI are lower than those of ZnO/PI. Figure 4 showed typical thermogravimetric profiles of $Zn(NO_3)_2$/PI films. As shown in Table I, the addition of only 5 mol % of $Zn(NO_3)_2$ into PI decreased the T_d by 17°C. However, adding more amounts of $Zn(NO_3)_2$/PI from 5 to 117.6 mol % dramatically decrease the T_d by 17 to

TABLE 1
The Degradation Temperature of Pure PI, ZnO/PI and Zn Nitrate/PI

ZnO content (mol %)	Zn nitrate/PI		ZnO/PI	
	T_d (°C)	ΔT_d (°C)	T_d (°C)	ΔT_d (°C)
Pure PI	555	–	555	–
0.6	–	–	535	−20
3.3	–	–	523	−32
5	538	−17	–	–
10	494	−61	–	–
15	484	−71	–	–
35.1	423	−132	520	−35
74.1	399	−156	508	−47
117.6	351	−204	505	−50

T_d was defined as T of material at 5 wt % loss.
$\Delta T_d = T_d - T_d$ (pure PI).

204°C. Figure 5 shows typical thermogravimetric profiles of ZnO/PI films. The T_d of these nanocomposites clearly decrease to a certain extent when adding ZnO nanoparticles directly into the films, as shown in Table I. Addition of 0.6–117.6 mol % of ZnO into PI films decreases the T_d by 20–50°C. Interestingly, the ZnO/PI and $Zn(NO_3)_2$/PI films prepared at the same 35.1 mol % concentration show different thermogravimetric profiles. The T_d of ZnO/PI decrease only by 35°C compared to 132°C in the case of $Zn(NO_3)_2$/PI. Obviously the ZnO/PI film has better thermal stability than the $Zn(NO_3)_2$/PI film. The difference between the T_d of ZnO/PI and that of $Zn(NO_3)_2$/PI film was a consequence of the origin of ZnO nanoparticles. Since metallic salts added into PI films induced acidic hydrolysis (chain scission) and oxidative degradation of polyimide,[12,13] the T_d of $Zn(NO_3)_2$/PI film decreased dramatically. This result was consistent with Hsu et al.'s [10] and Chiang and Whang's.[13]

The optical absorbance and fluorescence spectra observed for the PI films containing 35.1 mol % ZnO

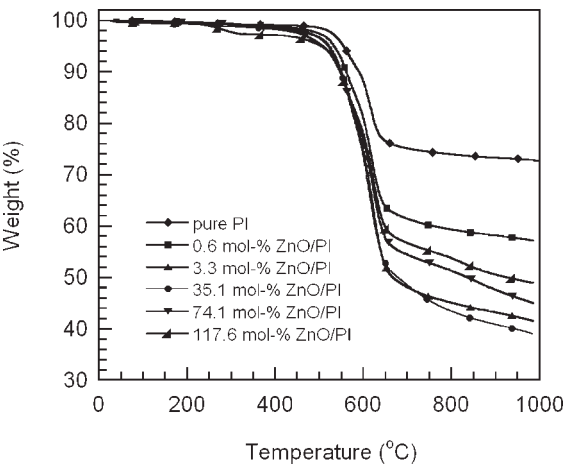

Figure 5 Thermogravimetric profiles of PI containing directly added ZnO nanoparticles.

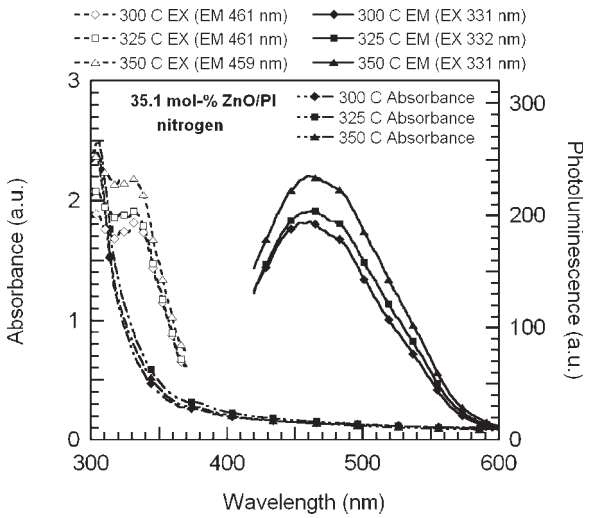

Figure 6 Effect of curing temperature on fluorescence of 35.1 mol % ZnO/PI cured under nitrogen atmosphere.

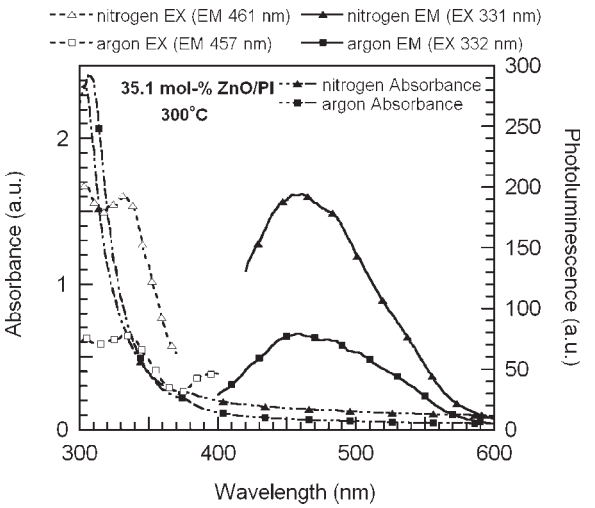

Figure 7 Effect of curing atmosphere on fluorescence of 35.1 mol % ZnO/PI cured at 300°C.

at different curing temperatures are shown in Figure 6. The characteristic peaks attributable to the exciton absorption of ZnO are observed at 305 nm for all the ZnO/PI films with different curing temperatures. The absorption spectra of all films are shown in the range of 305–410 nm, and the absorption was quenched above 410 nm. The emission peak of all films was located at 461 nm for both 300°C and 325°C curing temperatures and was slightly shifted to 469 nm for the film cured at 350°C. The intensity of emission slightly increased as the curing temperature increased. Though the data are not shown here, the effect of the curing temperature at a different fixed ZnO concentration exhibited a similar trend as the one just mentioned. Since the effect of curing temperature on the fluorescent intensity is slight, the curing temperature of 300°C was chosen to explore the effect on fluorescence.

Figure 7 shows the effects of curing atmosphere, nitrogen or argon, on the absorbance and fluorescence at room temperature of 35.1 mol % ZnO/PI films. The films were imidized at 300°C under either nitrogen or argon atmosphere. The exciton absorption peaks of the films cured under nitrogen and argon atmosphere are observed at 302 and 307 nm, respectively. The film prepared under nitrogen shows emission and excitation peaks at 461 and 331 nm, respectively. Similarly the film prepared under argon showed peaks at 457 and 332 nm, respectively. The emission peak of the former is slightly red shifted and exhibited 2.4 times higher intensity than the latter which is consistent with Roy et al.[16] ZnO synthesized under nitrogen emitted higher intensity of green light than that prepared under argon which could be due to different intrinsic defects in ZnO such as oxygen vacancy and interstitial zinc. The effect of the curing atmosphere at other ZnO concentrations exhibited similar trends (the spectra are not shown here).

The effects of ZnO concentration on the fluorescence and absorbance were presented in Figures 8–11. All the films were imidized at 300°C under nitrogen. As expected, the existence of ZnO in PI films enhanced the fluorescence emission. Figures 8 and 9 show the effect of ZnO/PI concentration on the optical absorption and emission intensity, respectively. As the concentration of ZnO nanoparticles increases from 0.6 to 117.6 mol %, Figure 8 shows that the exciton absorption peak is blue shifted from 318 to 295 nm and the absorbance decreased. This phenomenon is caused by the broadened distribution of aggregates of ZnO nanoparticles in the PI film, which was confirmed by TEM image (Fig. 13). All samples exhibited absorption spectra in the range of 300–370 nm. Above 370 nm, the absorbance of pure

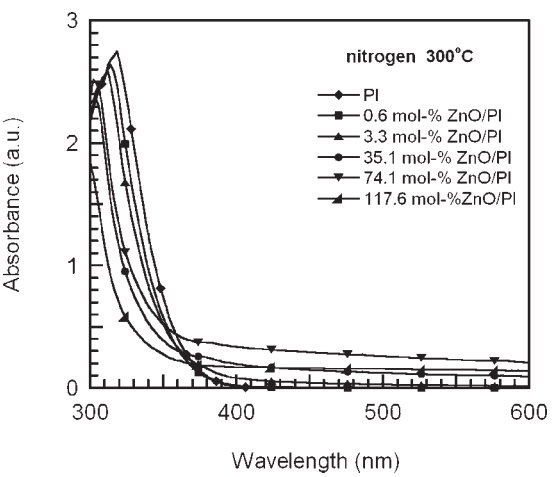

Figure 8 Effect of ZnO concentration on absorbance of ZnO/PI cured under nitrogen atmosphere at 300°C.

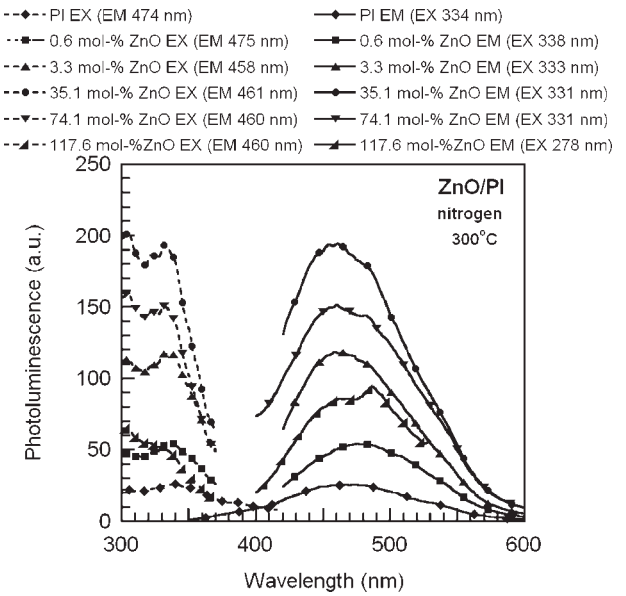

Figure 9 Effect of ZnO concentration on fluorescence of ZnO/PI cured under nitrogen atmosphere at 300°C.

PI, 0.6 and 3.3 mol % ZnO/PI films was quenched in the visible region. However, some incremental absorbance intensity in the visible region (above 370 nm) was detected in high-concentration ZnO/PI films (>35.1 mol % ZnO) due to the presence of submicron-size ZnO particles, which was confirmed by TEM micrograph (Fig. 13). The high-concentration ZnO/PI films are less transparent than the corresponding $Zn(NO_3)_2$/PI films because submicron-sized ZnO cause significant light scattering in the visible region.

Figure 9 shows that, as the concentration of ZnO nanoparticles increased to 3.3 mol %, the fluorescent intensity increased and was slightly blue shifted from 474 to 458 nm compared to that of pure PI, although the wavelength of the excitation peak of all films was approximately the same (except the case of 117.6 mol % ZnO). As the concentration of ZnO nanoparticles increased to 35.1 mol % and above, the fluorescent intensity is, however, not shifted further compared to that of 3.3 mol % ZnO/PI. More specifically, at 0.6 and 35.1 mol % of ZnO nanoparticles, the fluorescent intensity at visible wavelength was enhanced by 2.2 and 7.8 times compared to that of pure PI. However, adding more amounts of ZnO nanoparticles at 74.1 and 117.6 mol % to the films, the light emission intensity was dramatically decreased because of the self-absorption of ZnO. Fluorescence was generally inversely proportional to the concentration owing to the concentration quenching,[17] which can be classified into two categories: self-quenching and self-absorption. Self-quenching is a collision phenomenon between molecules in the ground state and those in excited state conditions, which leads to the energy transfer without fluorescence. On the other hand, self-absorption is a phenomenon in which the wavelength of fluorescence overlaps that of the absorption by the sample. In other words, the fluorescence was absorbed by the other molecules. This is consistent with the appearance of an increase in the absorption in the visible region (above 370 nm). Moreover, the emission in the visible region at all concentrations of ZnO nanoparticles except 0.6 mol % in PI films showed two main peaks at 460 and 485 nm, similar to the result by Roy et al.[16] The peak appearing at 485 nm could be originated from oxygen vacancy defect in ZnO.

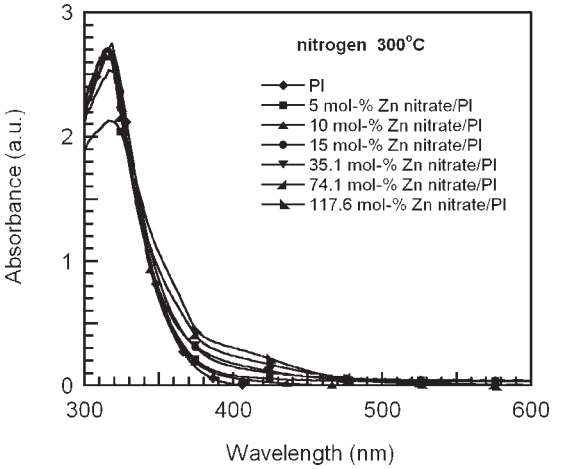

Figure 10 Effect of ZnO concentration on absorbance of Zn nitrate/PI cured under nitrogen atmosphere at 300°C.

Similarly, the effects of ZnO concentration from thermal decomposition of $Zn(NO_3)_2$ in PI films on the absorbance and fluorescence of Zn nitrate/PI films were shown in Figures 10 and 11, respectively.

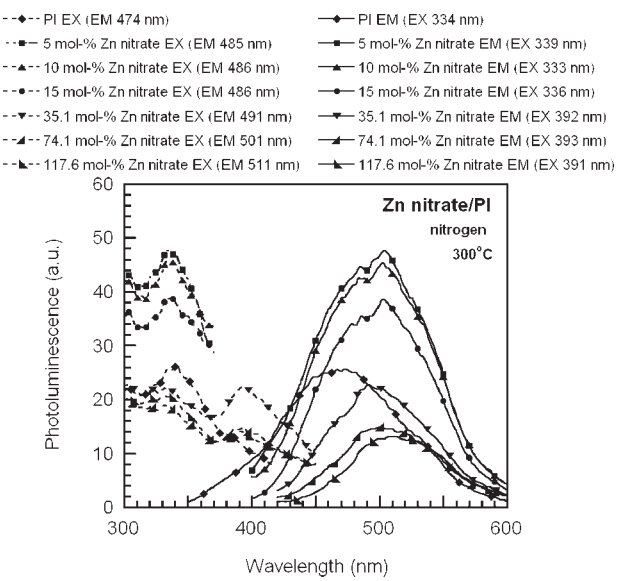

Figure 11 Effect of ZnO concentration on fluorescence of Zn nitrate/PI cured under nitrogen atmosphere at 300°C.

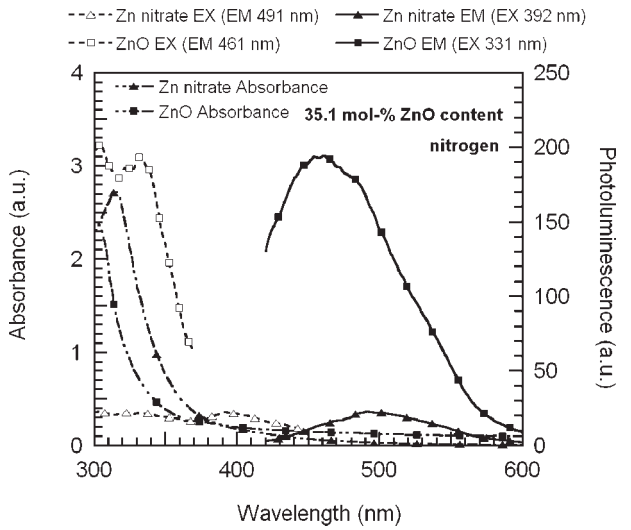

Figure 12 Effect of the origin of ZnO at concentration of 35.1 mol % on fluorescence cured under nitrogen atmosphere at 300°C.

In Figure 10, $Zn(NO_3)_2$/PI films of all concentrations exhibit broad absorption in the range of 300–370 nm with peaks around 318 nm. The absorption above 370 nm gradually increase as the concentration of $Zn(NO_3)_2$ increase due to the increase in particle size of ZnO as confirmed by XRD. However, the exciton absorption peak at all Zn nitrate concentrations was not shifted compared to that of the ZnO/PI films.

Figure 11 showed the effect of ZnO concentration in $Zn(NO_3)_2$/PI films on the fluorescent intensity and wavelength. Adding only 5 mol % of $Zn(NO_3)_2$ to the PI film shows the highest intensity in the visible region compared to all other concentrations. In fact, the fluorescent intensity of 5 mol % Zn nitrate/PI was 1.9 times that of the pure PI. On the other hand, the intensities of 10 and 15 mol % Zn $(NO_3)_2$/PI are lower than that of 5 mol % $Zn(NO_3)_2$/PI, whereas the fluorescent intensity of 35.1, 74.1, and 117.6 mol % $Zn(NO_3)_2$/PI films became even lower than that of pure PI as the concentration increases owing to the aggregation of ZnO nanoparticles. Moreover, the emission peak of these $Zn(NO_3)_2$/PI films was red shifted when compared to that of the pure PI films, which may also be attributed to the aggregation of ZnO nanoparticles. This result is consistent with the appearance of the increasing absorption above 370 nm. In contrast, the light emission of ZnO/PI was slightly blue shifted because of no change in the size of ZnO nanoparticles in the PI films, which was confirmed by TEM image (Fig. 13).

By the way, the visible light emission of 5, 10, and 15 mol % $Zn(NO_3)_2$/PI showed two main peaks at 486 and 502 nm, similar to the results reported by Roy et al.[16] In addition, all samples emitted green color. The visible light emission was assumed to be caused by different intrinsic defects in ZnO such as oxygen vacancy and interstitial zinc (450–600 nm).[18–20]

Figure 12 showed the effect of the origin of ZnO on the absorbance and fluorescence of PI films at the same ZnO concentration of 35.1 mol %. The films were imidized at 300°C under nitrogen. The exciton absorption peaks of $Zn(NO_3)_2$/PI and ZnO/PI are observed at 313 and 301 nm, respectively. Both PI films show absorption bands in the range of 300–400 nm. However, an increase in absorbance (above 400 nm) was observed for ZnO/PI compared to that of $Zn(NO_3)_2$/PI. Furthermore, the fluorescence of ZnO/PI shows an emission peak at 461 nm, which is significantly blue shifted from the 491 nm of $Zn(NO_3)_2$/PI, and also exhibits a much higher intensity. The excitation and emission peaks of ZnO/PI are enhanced by 8.7 times than those of $Zn(NO_3)_2$/

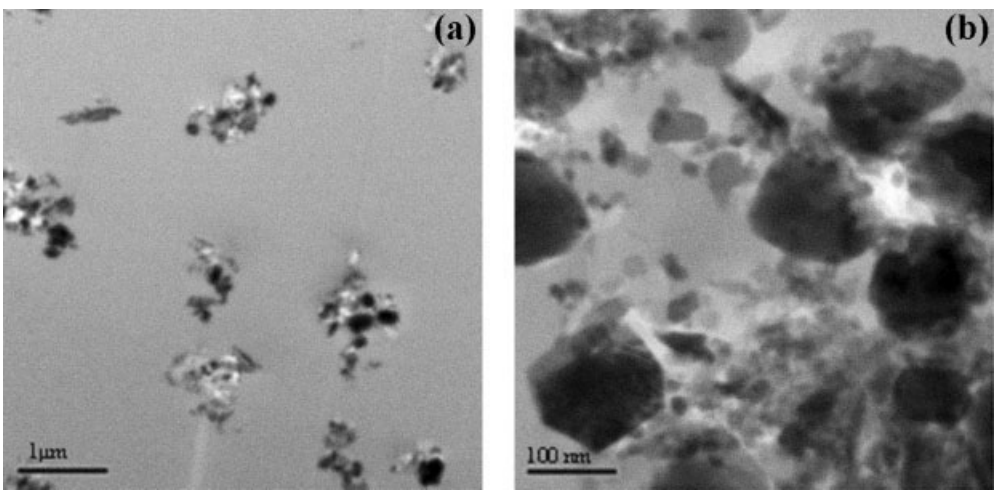

Figure 13 TEM images of polyimide containing 117.6 mol % ZnO nanoparticles (a) low magnification image (×12,000) (b) high magnification image (×120,000).

PI, which is attributed to an imperfect crystal structure and smaller crystallite sizes of ZnO nanoparticles in $Zn(NO_3)_2$/PI films (confirmed with XRD data). In addition, the ZnO generated from the thermal decomposition of $Zn(NO_3)_2$ in PI films results in more self-quenching than ZnO nanoparticles dispersed in ZnO/PI films.

The TEM images of 117.6 mol % ZnO/PI films are shown in Figure 13(a,b). Obviously the ZnO nanoparticles are well distributed throughout the film but poorly dispersed in PI films as can be seen in Figure 13(a). The diameter of ZnO primary particle obtained from the vendor is around 2 nm. The aggregates of ZnO nanoparticles with an average diameter of 17–90 nm are observed in Figure 13(b) and approximately agglomeration of ZnO nanoparticles with average size of 114–150 nm is also observed. However, small ZnO nanoparticles generated from the thermal decomposition of $Zn(NO_3)_2$ are not observed in this study mainly due to the limitation of TEM resolution capacity (data not shown).

CONCLUSIONS

The thermal conversion of zinc nitrate hexahydrate ($Zn(NO_3)_2{\cdot}6H_2O$) to zinc oxide (ZnO) nanoparticles was confirmed by XRD technique. The glass transition temperature (T_g) of ZnO nano-particle-dispersed polyimide films (ZnO/PI) slightly increase when the concentration of ZnO nanoparticles is higher than 35.1 mol %, which is due to the confinement of polymer chain mobility by ZnO. However, no T_g of $Zn(NO_3)_2$/PI were observed in the film. The 5 wt % degradation temperatures (T_d) of all nanocomposite films are lower than that of pure PI, though the ZnO/PI films exhibits higher thermal stability than $Zn(NO_3)_2$/PI films.

The 35.1 mol % ZnO/PI exhibits fluorescence with the highest intensity, which is 7.8 times as high as that of pure PI. In fact, the fluorescent intensities of all ZnO/PI films are higher than that of pure PI. An addition of only 5 mol % $Zn(NO_3)_2$ enhances the fluorescence by 1.9 times compared with that of pure PI. Moreover, the light emission of $Zn(NO_3)_2$/PI films shows a red shift compared to that of pure PI. This may be attributed to the aggregation of ZnO nanoparticles. As for the effect of the curing atmosphere on fluorescence, the films prepared under nitrogen emit higher fluorescent intensity than those prepared under argon. However, the curing temperature gives slightly effect on the fluorescent intensity. The TEM images show ZnO nanoparticles embedded in PI films in which the aggregates with an average diameter of 17–90 nm are observed. In addition, ZnO nanoparticles agglomerate with average size of 114–150 nm. In other words, ZnO nanoparticles are well distributed but poorly dispersed in the PI films. It is expected that the optical properties of the ZnO-containing PI films would be further enhanced if the ZnO nanoparticles could be uniformly distributed and dispersed as primary particles in the films.

The authors thank Dr. Toemsak Srikhirin, Department of Physics, Faculty of Science, Mahidol University for use of luminescence spectrometer and spectrophotometer for this study.

References

1. Ghosh, M. K.; Mittal, K. L. Polyimides Foundamentals and Applications; Marcel Dekker: New York, 1996.
2. Chiron, D.; Trigaud, T.; Moliton, J. P. Synthetic Met 2001, 124, 33.
3. Cornic, C.; Lucas, B.; Moliton, A.; Colombeau, B.; Mercier, R. Synthetic Met 2002, 127, 299.
4. Kim, J. H.; Koros, W. J.; Paul, D. R. Polymer 2006, 47, 3104.
5. Kim, H.; Horwitz, J. S.; Kim, W. H.; Mäkinen, A. J.; Kafafi, Z. H.; Chrisey, D. B. Thin Solid Films 2002, 539, 420.
6. Cembrero, J.; Elmanouni, A.; Hartiti, B.; Mollar, M.; Mari, B. Thin Solid Films 2004, 198, 451
7. Hirai, T.; Harada, Y.; Hashimoto, S.; Itoh, T.; Ohno, N. J lumin 2004, 112, 196.
8. Tsukazaki, A.; Ohtomo, A.; Onuma, T.; Ohtani, M.; Makino, T.; Sumiya, M.; Ohtani, K.; Chichibu, S. F.; Fuke, S.; Segawa, Y.; Ohno, H.; Koinuma, H.; Kawasaki, M. Nat Mater 2005, 4, 42.
9. Guo, L.; Yang, S.; Yang, C.; Yu, P.; Wang, J.; Ge, W.; Wong, G. K. L. Chem Mater 2003, 12, 2268.
10. Hsu, S. C.; Whang, W. T.; Hung, C. H.; Chiang, P. C.; Hsiao, Y. N. Macromol Chem Phys 2005, 206, 291.
11. Andelman, T.; Gong, Y.; Polking, M.; Yin, M.; Kuskovsky, I.; Neumark, G.; O'Brien, S. J Phys Chem B 2005, 109, 14314.
12. Sawada, T.; Ando, S. Chem Mater 1998, 10, 3368.
13. Chiang, P. C.; Whang, W. T. Polymer 2003, 44, 2249.
14. Chae, D. W.; Kim, B. C. Polym Adv Technol 2005, 16, 846.
15. Savin, D. A.; Pyun, J.; Patterson, G. D.; Kowalewski, T.; Matyjaszewski, K. J Polym Sci Pol Phys 2002, 40, 2667.
16. Roy, V. A. L.; Djurisic, A. B.; Chan, W. K.; Gao, J.; Lui, H. F.; Surya, C. Appl Phys Lett 2003, 83, 141.
17. Lawan, S. Fluorometric analysis; Faculty of Pharmaceutical Sciences Sillapakron University: Nakonpatom, 2544.
18. Lin, B.; Fu, Z.; Jia, Y. Appl Phys Lett 2001, 79, 943.
19. Lin, Y.; Xie, J.; Wang, H.; Li, Y.; Chavez, C.; Lee, S. Y.; Foltyn, S. R.; Crooker, S. A.; Burrell, A. K.; McCleskey, T. M.; Jia, Q. X. Thin Solid Films 2005, 492, 101.
20. Masuda, Y.; Kinoshita, N.; Sato, F.; Koumoto, K. Cryst Growth Des 2006, 6, 75.